Auditory ganglion source of Sonic hedgehog regulates timing of cell cycle exit and differentiation of mammalian cochlear hair cells

Jinwoong Bok[a,1,2], Colleen Zenczak[b,1], Chan Ho Hwang[b,3], and Doris K. Wu[b,2]

[a]Department of Anatomy, Department of Otorhinolaryngology, BK21 Project for Medical Science, Yonsei University College of Medicine, Seoul, 120-752, Korea and [b]Laboratory of Molecular Biology, National Institute on Deafness and Other Communication Disorders, Rockville, MD 20850

Edited by Huda Y. Zoghbi, Jan and Dan Duncan Neurological Research Institute, Texas Children's Hospital, Houston, TX, and approved July 12, 2013 (received for review December 28, 2012)

Neural precursor cells of the central nervous system undergo successive temporal waves of terminal division, each of which is soon followed by the onset of cell differentiation. The organ of Corti in the mammalian cochlea develops differently, such that precursors at the apex are the first to exit from the cell cycle but the last to begin differentiating as mechanosensory hair cells. Using a tissue-specific knockout approach in mice, we show that this unique temporal pattern of sensory cell development requires that the adjacent auditory (spiral) ganglion serve as a source of the signaling molecule Sonic hedgehog (Shh). In the absence of this signaling, the cochlear duct is shortened, sensory hair cell precursors exit from the cell cycle prematurely, and hair cell differentiation closely follows cell cycle exit in a similar apical-to-basal direction. The dynamic relationship between the restriction of *Shh* expression in the developing spiral ganglion and its proximity to regions of the growing cochlear duct dictates the timing of terminal mitosis of hair cell precursors and their subsequent differentiation.

morphogenesis | *Atoh1* | tonotopy

The mammalian cochlea, a coiled sensory end organ of hearing, contains a specialized mechanosensory epithelium (organ of Corti) consisting of hair cells (HCs) and nonsensory supporting cells. Sound frequency discrimination in mammals begins in the cochlea with a frequency-place code, such that specific frequencies elicit maximal responses of the organ of Corti at different points along its longitudinal (basal-apical) axis, a phenomenon known as tonotopy. Many structural and molecular features of the mature organ of Corti that vary along the longitudinal (tonotopic) axis, including stiffness of the basilar membrane and size and shape of the sensory HCs and their associated stereocilia (1, 2), have been implicated as contributing factors in frequency discrimination. The developmental bases of tonotopy remain obscure, however (3).

A possible developmental influence on tonotopy is the well-characterized dynamic of apical (low-frequency sensing) precursors exiting early from the cell cycle, evident at embryonic day (E) 12.5 in mice, followed by a wave-like spread of terminal mitosis toward the base (high-frequency sensing), with cells completing cell cycle exit (CCE) by E14.5 (Fig. 1*A*) (4, 5). In contrast, early markers of HC differentiation, such as *atonal homolog 1* (*Atoh1*), first appear at the midbase at E13.5 and spread bidirectionally along the developing organ of Corti (Fig. 1*A*) (6). Consequently, apically located HC precursors remain in a postmitotic, undifferentiated state for a longer period than their more basal counterparts. This unusual pattern of cellular regulation is in stark contrast to the neural precursors in the cortex and retina, in which each neuronal subtype has a specific timing of terminal mitosis, followed closely by its differentiation (7, 8).

Gradients of secreted molecules are important for patterning and cell fate specification during embryogenesis. Although these gradients are thought to be established by diffusion of the secreted molecules across the tissue from a restricted source, mechanisms that maintain these gradients are not well understood and are under active investigation (9). Conceivably, morphogenetic changes in response to the secreted molecules can also modify or limit the extent of signaling received by target cells. However, few clear examples of sequential integration of cell signaling-morphogenesis-cell signaling have been described in vertebrates.

Shh secreted from the notochord and floor plate are required for patterning in the cochlea (10–12). Additionally, Shh is expressed in the spiral ganglion that innervates cochlear HCs, and studies conducted using a *Shh-cre-Gfp* reporter strain indicate that *Shh* expression in the developing spiral ganglion becomes concentrated near the apex of the growing cochlear duct over time (13). Given that Shh has been shown to inhibit HC formation in cochlear explants (14), the restriction of *Shh* reporter expression in the spiral ganglion has been postulated to regulate cochlear HC differentiation in vivo, even though the reporter activities appear to be ubiquitously high at the onset of HC differentiation (13). If Shh signaling indeed blocks HC formation in vivo, then loss of *Shh* in the spiral ganglion should result in HCs at the apex differentiating promptly after CCE, similar to other neural and sensory systems (7, 8). This prediction also requires that *Shh* be uninvolved in regulating the timing of CCE of prospective HCs. To test this hypothesis, we investigated in detail *Shh* expression and signaling during mouse cochlear development, and analyzed the timing of CCE and HC differentiation in cochleae with targeted deletion of *Shh* in the spiral ganglion. Our results show that integration of Shh signaling from the spiral ganglion and morphogenesis of the cochlear duct dictate the timing of HC precursors exit from cell cycle and subsequent HC differentiation within the cochlea.

Results

Restriction of *Shh* Expression in the Spiral Ganglion During Cochlear Duct Outgrowth. We investigated Shh signaling in the developing cochlea and extended the *Shh* reporter studies by examining mRNA transcripts of *Shh* and *Patched1* (*Ptc1*), a gene activated by Shh (15), during cochlear development. *Shh* transcripts were first detected in a subpopulation of cells within the cochleovestibular ganglion (CVG) starting at E11.75 (Fig. 1*B*), earlier than reported previously (13). However, similar to the previous study, these cells were located in the part of the spiral ganglion that is closely associated with the apex of the cochlea by E15.5

Author contributions: J.B., C.Z., C.H.H., and D.K.W. designed research; J.B., C.Z., and C.H.H. performed research; J.B., C.Z., C.H.H., and D.K.W. analyzed data; and J.B., C.Z., and D.K.W. wrote the paper.

The authors declare no conflict of interest.

This article is a PNAS Direct Submission.

Freely available online through the PNAS open access option.

[1]J.B. and C.Z. contributed equally to this work.

[2]To whom correspondence may be addressed. E-mail: bokj@yuhs.ac or wud@nidcd.nih.gov.

[3]Present address: Yangcheon Seoul ENT Clinic, 49 Mokdong-seoro, Yangcheon-gu, Seoul 158-878, South Korea.

This article contains supporting information online at www.pnas.org/lookup/suppl/doi:10.1073/pnas.1222341110/-/DCSupplemental.

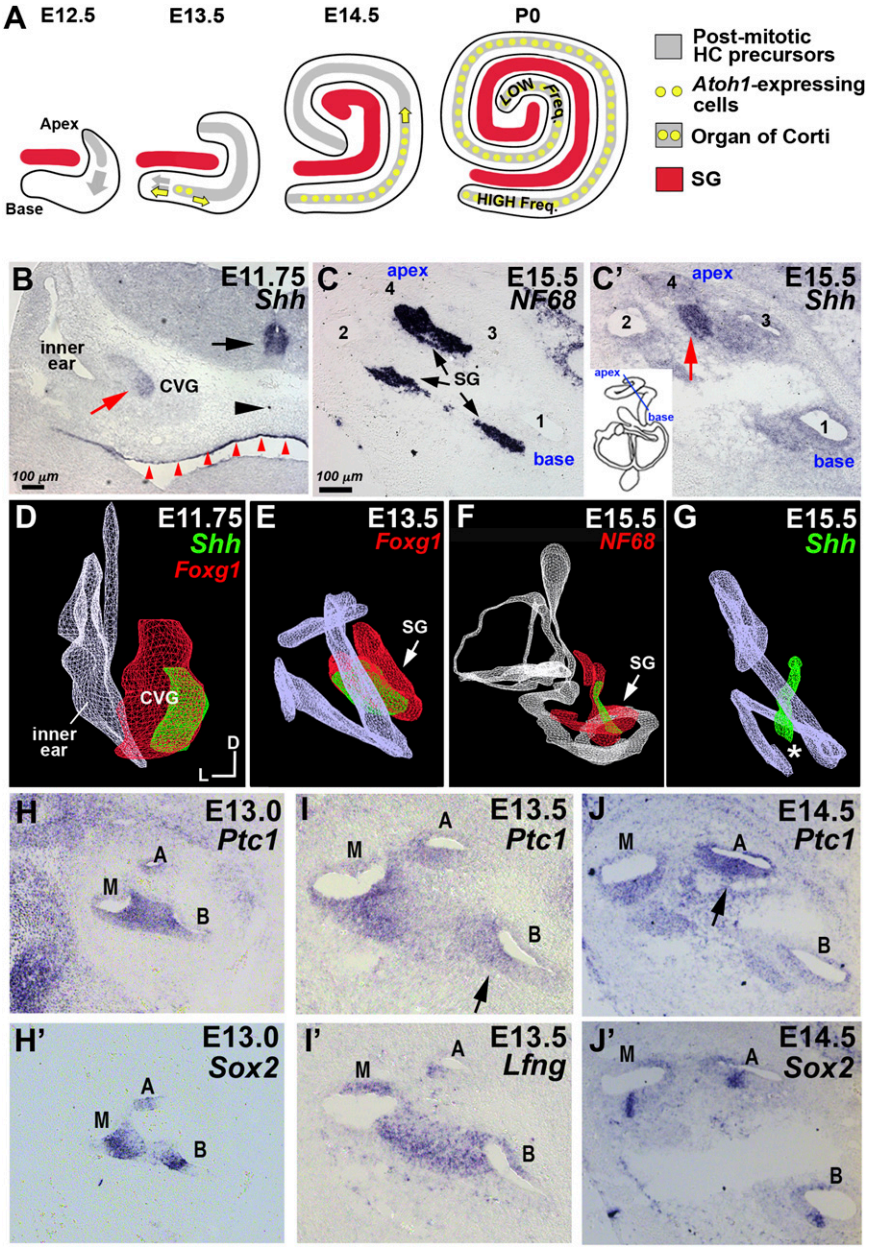

Fig. 1. Expression of *Shh* in the developing spiral ganglion and *Ptc1* in the cochlear duct. (*A*) In mouse cochlea, HC precursors at the apex start exiting from the cell cycle at E12.5, whereas HC differentiation starts at the midbase at E13.5 and progresses bidirectionally along the duct. (*B*) *Shh* is expressed in the CVG (red arrow), floor plate (black arrow), notochord (black arrowhead), and pharyngeal endoderm (red arrowheads). (*C* and *C′*) Adjacent cochlear sections showing *Shh* expression in a subset of neurofilament-positive (*NF68*) spiral ganglion (SG) neurons (black arrows) associated with the apical turn of the cochlear duct (red arrow). (*D–G*) Posterior views of 3D images of inner ears (*D* and *F*) and cochleae (*E* and *G*). *Shh* expression (green) in the *Foxg1*$^{+}$ (*D* and *E*) or *NF68*$^{+}$ (*F*) spiral ganglion (red) was gradually restricted by the apex of the cochlear duct over time (asterisk). (*H–J′*) *Ptc1* expression ($n = 10$) is weak in the apex of the *Sox2*$^{+}$ prosensory domain at E13 (*H* and *H′*), reduced at the basal prosensory region at E13.5 (*I* and *I′*, arrow), and strongest at the apex (arrow) by E14.5 (*J* and *J′*, arrow). A, apex; B, base; M, mid, D, dorsal; L, lateral.

(Fig. 1 *C* and *C′*). Three-dimensional reconstruction of *Shh* expression patterns between E11.5 and E15.5 indicated that as the spiral ganglion follows the contour of the growing cochlear duct over time (Fig. 1 *D–F*, red), the subpopulation of *Shh*$^{+}$ cells in the ganglion appears to restrict and converge toward the apex of the cochlear duct (Fig.1 *D–G*, green, asterisk). Analyses of *Ptc1* expression indicated that Shh signaling received by the developing cochlea is initially stronger at the base and mid region of the *Sox2* and *Lunatic fringe* (*Lfng*)$^{+}$ prosensory domain at E13.0 (Fig. 1 *H* and *H′*), but starts to decrease at the base within 0.5 d (Fig. 1 *I* and *I′*) and becomes restricted to the apex by E14.5 (Fig. 1 *J* and *J′*). The timing of base-to-apex reduction of Shh signaling is consistent with the known timing of HC differentiation (6).

Cochlear Duct Growth Depends on *Shh* Signaling from the Spiral Ganglion. To determine whether *Shh* produced by the spiral ganglion affects cochlear development, we generated ganglion-specific knockouts using three different cre strains: *Foxg1*^{Cre}, *Ngn1*^{Cre}, and *Ngn1*^{CreERT2} (16–18). *Neurogenin1* (*Ngn1*) expression is initiated in neuroblasts of the CVG before their delamination from the otic epithelium (19). *Foxg1* is expressed in the otocyst and CVG (16). Based on published *cre* reporter activities, all three cre strains should ablate *Shh* expression in the CVG (16–18) while sparing its expression in the notochord and floor plate, two sources of Shh thought to be required for specification of cochlear identity (10, 11).

Whereas conditional knockout mutants generated using these three *cre* strains showed intact *Shh* expression in the notochord and floor plate, deletion of *Shh* expression in the CVG was more complete when using *Foxg1*^{Cre} compared with *Ngn1*^{CreERT2} or *Ngn1*^{Cre} (Figs. S1 and S2). In the *Foxg1*^{Cre}; *Shh*$^{lox/-}$ mutants, some *Shh* expression was detected in the CVG between E11.5 and E13.5 (Figs. S1*H* and S6*C*), but very little of this ganglionic tissue reached the developing cochlea at E13.5 and E15.5 (Figs. S1 *B* and *F* and S6 *D* and *D′*). In contrast, both *Ngn1*^{Cre}; *Shh*$^{lox/-}$ and *Ngn1*^{CreERT2}; *Shh*$^{lox/-}$ mutants showed a similar pattern of *Shh* restriction in the spiral ganglion as controls, but the expression domain was reduced in the mutants by E15.5 (Figs. S1*L* and S2

G and *H*). These results are further supported by the expression patterns of *Ptc1* (Figs. S1 and S2). In addition, *Shh* expression in the pharyngeal endoderm of *Foxg1*^{Cre}; *Shh*$^{lox/-}$ mutants was absent (Fig. S1), consistent with the expression of *Foxg1* in this tissue (16).

We next analyzed the gross anatomy of *Shh* conditional mutants using the paint-fill technique. In the most severe *Shh* conditional mutants, *Foxg1*^{Cre}; *Shh*$^{lox/-}$, the cochlear duct consisted of only one-half of a turn (Fig. 2*A* and *B*). In the milder *Ngn1*^{CreERT2}; *Shh*$^{lox/-}$ conditional mutant, the cochlear duct was shorter, with its length dependent on whether tamoxifen administration for activating cre-mediated recombination began at E9.5 or at E10.5 (Fig. 2 *C*–*E*). These results indicate that *Shh* from the spiral ganglion dictates cochlear duct length.

Premature Sensory Hair Cell Differentiation in the *Ngn1*^{Cre};*Shh*$^{lox/-}$ Cochlea. To address our hypothesis that Shh regulates the wave of HC differentiation in the cochlea, we analyzed the timing of HC differentiation and its relationship to CCE in the *Shh* conditional mutants. We focused on HC development in the *Ngn1*^{Cre};*Shh*$^{lox/-}$ mutants, which survive the longest of the three strains of conditional mutants used. *Atoh1,* one of the earliest genes associated with HC fate, was first detected in the midbasal region of *Ngn1*^{Cre}; *Shh*$^{lox/+}$ cochlea at E13.5 (Fig. 3*A*, white arrowheads), and this expression domain soon expanded bidirectionally along the cochlear duct, preceding the normal wave of HC differentiation (Fig. 1*A*) (6). In the mutant cochlea, *Atoh1* expression was strongly up-regulated in all regions except in the most apical region (Fig. 3*B*). This up-regulation of *Atoh1* was followed by premature cochlear HC differentiation examined between E15.5 and E18.5. At E15.5, normal nascent HCs stained with phalloidin showed thickened cortical actin condensations even though their stereocilia were barely visible. In control cochleae, one row of inner HCs (IHCs) and three rows of outer HCs (OHCs) were apparent in the basal region (Fig. 3*E*, arrowhead and bracket), whereas only immature IHCs were observed in the midregion (Fig. 3*F*, arrowhead). No cortical condensations were apparent in the apex at this stage (Fig. 3*G*) (20). Phalloidin staining showed a similar base-to-apex gradient of HC differentiation in *Ngn1*^{Cre}; *Shh*$^{lox/-}$ cochleae, except that HCs in the middle and apical cochleae of mutants appeared more mature compared with controls, with both IHCs and OHCs displaying thickened, actin-rich cortices (Fig. 3 *I* and *J*, arrowhead and bracket). The difference between basal mutant and control cochleae was not apparent at this age based on phalloidin staining (Fig. 3 *E* and *H*).

To better assess HC maturity at the base, we used anti–γ-tubulin antibodies to label the basal bodies and mark kinociliary locations within the HC. During HC maturation, the kinocilium moves from the center of the cell apex toward its edge before acquiring a final polarized, abneural position (21). Quantitative analyses of the basal cochlea showed increased numbers of mutant HCs with a kinocilium in the final polarized location compared with *Ngn1*^{Cre}; *Shh*$^{lox/+}$ controls (Fig. 3*C*). At subsequent ages, the premature HC differentiation phenotype in the mutants became progressively less evident at the base and midregion and was apparent only at the apex of the cochlea. Taken together, these results indicate that HC differentiation in the *Ngn1*^{Cre}; *Shh*$^{lox/-}$ cochlea progresses in a base-to-apex fashion as in normal controls, but does so prematurely. Although *Atoh1* up-regulation was also observed in the *Ngn1*^{CreERT2}; *Shh*$^{lox/-}$ cochlea (Fig. S2 *N* and *P*), HC differentiation was not assessed in these mutants owing to embryonic lethality beginning at E14.5, likely due to tamoxifen toxicity.

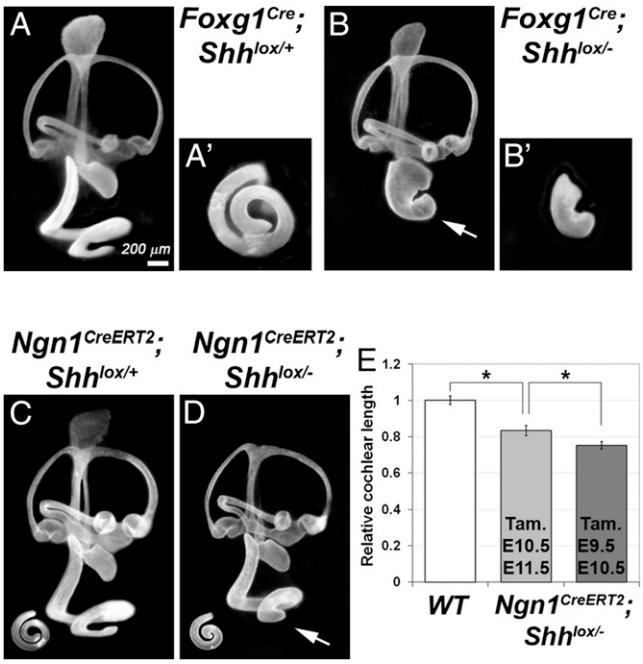

Fig. 2. Shortened cochlea in *Foxg1*^{Cre}; *Shh*$^{lox/-}$ and *Ngn1*^{CreERT2}; *Shh*$^{lox/-}$ mutants. (*A*–*D*) Paint-filled inner ears of E15.5 *Foxg1*^{Cre}; *Shh*$^{lox/+}$ (*A*), *Foxg1*^{Cre}; *Shh*$^{lox/-}$ (*B*), *Ngn1*^{CreER}; *Shh*$^{lox/+}$ (*C*), and *Ngn1*^{CreER}; *Shh*$^{lox/-}$ (*D*) embryos. (*A*′ and *B*′) Ventral view of the cochlea. In *B* and *D*, the arrow points to the shortened cochlea. (*E*) The length of the *Ngn1*^{CreER}; *Shh*$^{lox/-}$ cochlear duct is dependent on whether tamoxifen (Tam) is administered at E10.5 and E11.5 (light gray) or at E9.5 and E10.5 (dark gray). *$P < 0.0001$. The scale bar in *A* applies to *B*–*D* as well.

Moderate Premature Cell Cycle Exit of Hair Cell Precursors in *Ngn1Cre; Shh*$^{lox/-}$ Cochlea. To determine whether premature HC differentiation in *Ngn1*^{Cre}; *Shh*$^{lox/-}$ cochlea is caused by premature CCE, we conducted CCE analyses of sensory HCs by injecting pregnant females with the thymidine analog 5-ethynyl-2′-deoxyuridine (EdU) at specific times between E11.5 and E14. Mice were harvested at birth, when HCs are clearly identifiable using anti-myosin VIIa antibody. EdU^{+} HCs at the time of harvest are interpreted as having arisen from mitotic precursors at time of injection. Compared with control, the cochlear duct of the *Ngn1*^{Cre}; *Shh*$^{lox/-}$ mutants was 18.2% shorter (*Ngn1*^{Cre}; *Shh*$^{lox/+}$, mean 4,685 ± 335.29 μm; $n = 15$; *Ngn1*^{Cre}; *Shh*$^{lox/-}$, mean 3,832 ± 235.85 μm; $n = 14$; $P < 0.0001$) and contained 28% fewer HCs (Fig. S3). Cochlear duct lengths were parsed into nine equal bins for both mutants and controls (based on percentage of total length), and ratios of EdU-labeled HCs to total HCs were quantified for each bin. We found evidence of an apical-to-basal wave of CCE of HCs in control cochleae (Fig. S4*A*), comparable to that defined previously by ^{3}H-thymidine and BrdU labeling (4, 5). These results confirm that CCE in the organ of Corti begins at the apex around E12.5 and is completed at the base by E14.5.

Only a moderate reduction in the ratio of EdU-labeled HCs was detected in the basal cochlea of *Ngn1*^{Cre}; *Shh*$^{lox/-}$ specimens compared with controls after EdU injection at E13.5 and E14.0 (Fig. 3 *K* and *L*, asterisk and Fig. S4*B*). These results indicate that premature HC differentiation in *Ngn1*^{Cre}; *Shh*$^{lox/-}$ cochlea occurs with only a moderate change in CCE.

Premature Cell Cycle Exit of Hair Cell Precursors in the *Foxg1*^{Cre}; *Shh*$^{lox/-}$ Cochlea. We next sought to determine whether preservation of the normal (albeit premature) base-to-apex wave of HC differentiation in *Ngn1*^{Cre}; *Shh*$^{lox/-}$ cochleae is related to the presence of reduced *Shh* expression in the spiral ganglion (Fig. S1*L*), or whether *Shh* emanating from the ganglion is responsible for the timing, but not the directionality, of HC differentiation. To address this question, we conducted detailed investigations of *Foxg1*^{Cre}; *Shh*$^{lox/-}$ mutants, which demonstrate the greatest reduction of *Shh* expression in the spiral ganglion among all conditional mutants analyzed.

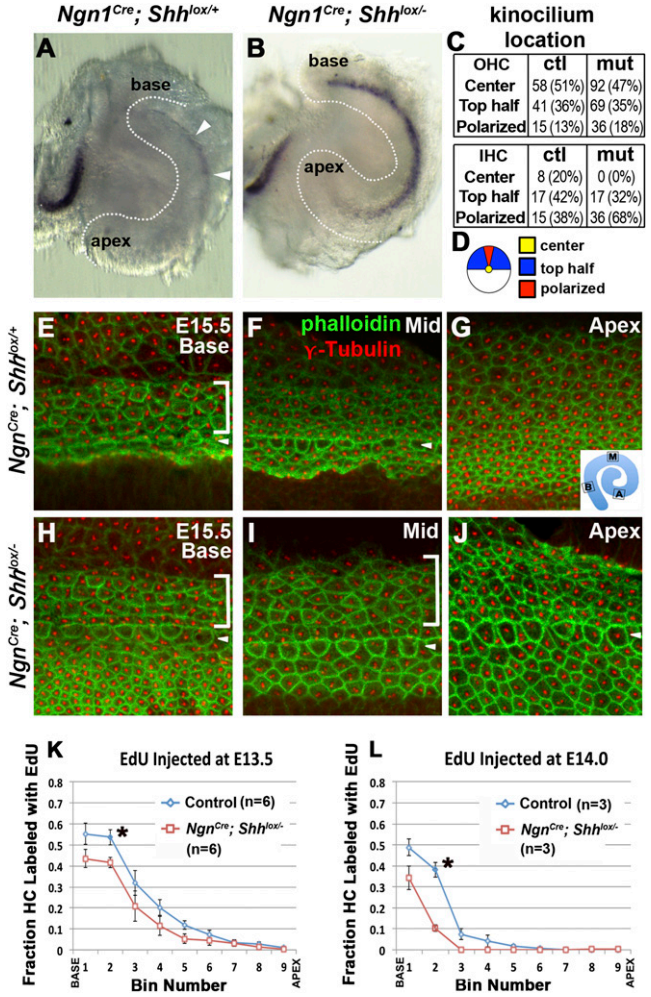

Fig. 3. Premature *Atoh1* expression and HC development but mild premature CCE in *Ngn1*^{Cre}*; Shh*$^{lox/-}$ cochlea. (*A* and *B*) Whole-mount in situ hybridization of *Ngn1*^{Cre}*; Shh*$^{lox/+}$ (*A*) and *Ngn1*^{Cre}*; Shh*$^{lox/-}$ (*B*) cochlea at E13.5. *Atoh1* is expressed at the midbase of the *Ngn1*^{Cre}*; Shh*$^{lox/+}$ cochlea (arrowheads), whereas its expression is strongly up-regulated in the *Ngn1*^{Cre}*; Shh*$^{lox/-}$ cochlea ($n = 4$). (*C*) Table presenting the number and percentages (brackets) of HCs with kinocilium (anti–γ-tubulin antibody) in indicated locations (defined in *D*) of control (*E*) and mutant (*H*) basal cochleae (bin 2). Nascent HCs initially display a centrally located kinocilium (yellow) that later migrates through the top half of the cell (blue) before arriving at its final position at the lateral edge (red). More HCs with polarized kinocilia are seen in *Ngn1*^{Cre}*; Shh*$^{lox/-}$ cochleae (*H*) compared with control cochleae (*E*) (OHC, $P = 0.015$; IHC, $P = 0.002$; χ^2 test with Yates' correction). (*E–J*) Luminal surface of *Ngn1*^{Cre}*; Shh*$^{lox/+}$ (*E–G*) and *Ngn1*^{Cre}*; Shh*$^{lox/-}$ (*H–J*) cochleae at the basal (*E* and *H*), mid (*F* and *I*), and apical (*G* and *J*) regions of the organ of Corti showing stereocilia labeled with phalloidin (green) and basal bodies labeled with anti–γ-tubulin (red; $n = 3$). Arrowheads and brackets point to cortical condensation of IHC and OHC, respectively. (*K* and *L*) Comparison of fraction of EdU-labeled HCs in *Ngn1*^{Cre}*; Shh*$^{lox/+}$ and *Ngn1*^{Cre}*; Shh*$^{lox/-}$ cochleae that were injected with EdU at E13.5 (*K*) and E14 (*L*). *$P < 0.05$. Error bars represent SEM.

The *Foxg1*^{Cre}*; Shh*$^{lox/-}$ cochlea did not show an exorbitant amount of apoptotic cells in the sensory domain during development, but contained only 20% of the normal amount of HCs. This reduction is most likely related to the severely shortened duct (Fig. S3). The disparity in cochlear length between mutants and controls makes direct quantitative comparisons of CCE difficult. Nonetheless, an end-stage analysis of *Foxg1*^{Cre}*; Shh*$^{lox/-}$ cochleae at E18.5 that were injected with EdU at E12.5 and E13.5 found fewer EdU-labeled HCs at the apex than in the base, suggesting preservation of the normal apex-to-base wave of CCE in these mutants (Fig. 4*A*). However, most HCs exited from the cell cycle by E13.5. Furthermore, qualitative analyses of specimens injected with EdU at E13.5 indicated that neither IHCs nor OHCs were EdU$^+$ at the apex (Fig. 4 *B*, mutant on the right in white and *E*). At the mid region, only OHCs are labeled (Fig. 4 *B*, light green and *D*), whereas the rest of the cochlear duct showed EdU labeling in both cell types (Fig. 4 *B*, green, and *C*). This labeling pattern is consistent with the dual dynamics of an apex- to-basal wave of CCE and IHCs exiting from the cell cycle before OHCs (Fig. 4*B*) (4, 5). Taken together, these results suggest that terminal mitosis of HC precursors in the *Foxg1*^{Cre}*; Shh*$^{lox/-}$ cochlea is premature, but an apical-to-basal wave of CCE is preserved.

Hair Cell Differentiation Proceeds in Apex to Base Direction in the *Foxg1*^{Cre}*; Shh*$^{lox/-}$ Cochlea. The direction of HC differentiation was reversed in the *Foxg1*^{Cre}*; Shh*$^{lox/-}$ cochlea compared with control and *Ngn1*^{Cre}*; Shh*$^{lox/-}$ cochleae. Phalloidin staining of *Foxg1*^{Cre}*; Shh*$^{lox/-}$ cochlea at E14.5 identified multiple rows of nascent HCs with a thickened cortical condensation in the apex (Fig. 4 *F* and *I*), with the phalloidin signal tapering off to a single row of less-mature HCs toward the base (Fig. 4 *F* and *H*, arrowheads). The saccule by the basal cochlea contained many more mature HCs with stereocilia (Fig. 4*G*). At 0.5 d later, HCs were more mature in the cochlea, and many more with distinct stereocilia were evident at the apex than at the base (Fig. 4 *M* and *N*, arrowheads). In contrast, no cortical condensation at E14.5 and only a single row of IHCs in the midbasal region at E15 of stage-matched littermate controls were observed (20).

Immunostaining for myosin VI, a marker of nascent HCs, showed a similar apical-to-basal gradient in the mutant cochlea as phalloidin staining (Fig. 4*J*). In stage-matched littermate controls, only a few cells with myosin VI immunoreactivity per cochlea were detectable in the midbase (Fig. 4 *K* and *L*), consistent with the aforementioned pattern of normal HC differentiation. By E18.5, most HCs in the normal cochlea had differentiated stereocilia, with the exception of those at the apex (Fig. S5*A*), whereas the *Foxg1*^{Cre}*; Shh*$^{lox/-}$ cochlea at this stage had HCs with differentiated stereocilia along its entire length (Fig. S5*B*).

Consistent with these morphological results, *Atoh1* expression at an early stage (E13) was present only in the apex of mutant cochlea (Fig. 5 *A–C*), in contrast to control cochleae, in which *Atoh1* expression was not detectable at this age. Taken together, these results suggest that in mutants, the normal pattern of HC differentiation (starting at the midbase and radiating longitudinally in both directions) is replaced by an apical-to-basal wave of HC differentiation that is initiated and completed prematurely.

Apical Region Is Present in *Foxg1*^{Cre}*; Shh*$^{lox/-}$ Cochlear Duct. It has been shown that cochlear duct patterning requires a gradient of Shh signaling that is highest at the apex and lowest at the base (11). This graded Shh signal has been attributed to the otocyst's proximity to the notochord and floor plate. However, the shortened cochlear duct in *Foxg1*^{Cre}*; Shh*$^{lox/-}$ mutants suggests the possibility that Shh secreted by the spiral ganglion provides additional Shh-mediated cues that pattern the apical cochlear duct, and this shortened cochlear duct represents a truncation that lacks the apical portion rather than a globally shortened structure. This scenario would confound our interpretation of an apical-to-basal wave of differentiation in the mutants.

We investigated this possibility by analyzing the *Foxg1*^{Cre}*; Shh*$^{lox/-}$ inner ears for expression of *Msx1*, a marker for the apical region of the cochlear duct (11). Our results show that *Msx1* expression in *Foxg1*^{Cre}*; Shh*$^{lox/-}$ mutants is comparable to that in controls at both E11.5 and E15.5 (Fig. 5 *D–G*), suggesting that the cochlear duct in *Foxg1*^{Cre}*; Shh*$^{lox/-}$ ears is not truncated, but is instead globally shortened. This finding further supports the idea that the progression of HC differentiation is inverted in the absence of Shh.

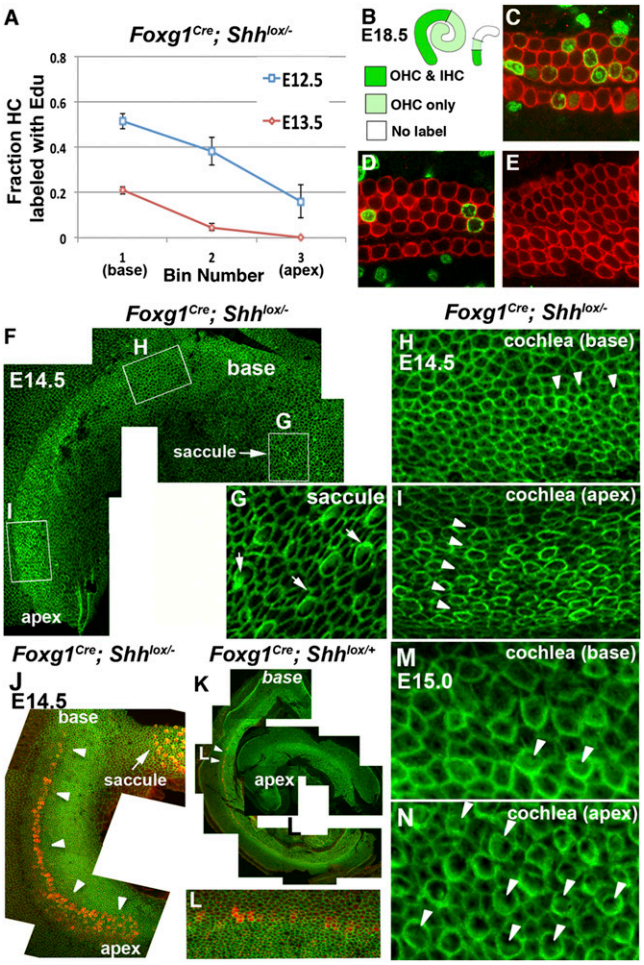

Fig. 4. EdU analysis and HC maturity of *Foxg1*^{Cre}; *Shh*$^{lox/-}$ cochlea. (*A*) Comparison of fraction of HCs labeled with EdU at the base, mid, and apex of E18.5 *Foxg1*^{Cre}; *Shh*$^{lox/-}$ cochleae that were injected with EdU at E12.5 and E13.5. (*B*) Traced confocal images of EdU labeling of control (*Left*, mean length 3,517 ± 262.89 μm; $n = 7$) and *Foxg1*^{Cre}; *Shh*$^{lox/-}$ (*Right*, mean length 678 ± 318.11 μm; $n = 4$) E18.5 cochlea after EdU injection at E13.5. Dark-green, light-green, and white regions represent EdU labeling in both IHCs and OHCs (*C*), in OHCs only (D), and in neither type of HCs (*E*), respectively. (*F–I*) Whole-mount preparation of an E14.5 *Foxg1*^{Cre}; *Shh*$^{lox/-}$ mutant cochlea labeled with phalloidin (green) showing more HCs with stronger actin condensation in the apex (*I*) than the base (*H*, arrowheads; $n = 4$). Also shown is the saccule displaying many distinct stereocilia-containing HCs (*G*, arrows). (*M* and *N*) More mature HCs with stereocilia are observed in the apex (*N*) than in the base (*M*) of *Foxg1*^{Cre}; *Shh*$^{lox/-}$ cochleae at E15.5 (arrowheads; $n = 2$). (*J–L*) Double-labeling of E14.5 *Foxg1*^{Cre}; *Shh*$^{lox/-}$ cochlea (*J*) with phalloidin (green) and anti-myosin VI antibodies (red) shows stronger myosin VI staining at the apex than at the base (arrowheads), whereas only weak myosin VI immunoreactivity is detectable at the midbase of control cochlea ($n = 2$). A similar pattern is observed with anti-myosin VII staining.

Discussion

We previously reported that Shh from the notochord and floor plate are important for regional patterning of the cochlea. The distal cochlear duct (closest to the ventral midline) requires robust Shh signaling, whereas the proximal end requires the least Shh signaling (11). The results of the present study indicate that the main function of Shh in the spiral ganglion is not in regional patterning of the cochlea, but rather in mediating cochlear growth and regulating the timing of CCE and HC differentiation. Despite the fact that Shh signaling is reduced in both the spiral ganglion and pharyngeal endoderm of the *Foxg1*^{Cre}; *Shh*$^{lox/-}$ mutants, we attributed most of the observed phenotypes to a lack of *Shh* in the spiral ganglion, given that an up-regulation of *Atoh1* in the cochlear apex similar to that reported here has been described in an analysis of the *Ngn1* null cochlea, which lacks a spiral ganglion (22).

Of note, the reverse gradient of HC differentiation was observed only in the *Foxg1*^{Cre}; *Shh*$^{lox/-}$ mutants, in which most spiral ganglion neurons failed to reach the developing cochlea (Figs. S1 and S6), and not in the other two *Shh* conditional mutants, in which some level of *Shh* reached the cochlear apex (Figs. S1 and S2). These results are consistent with our postulated role of *Shh* in the spiral ganglion. Considering that the spiral ganglion is essentially absent in both *Ngn1* nulls and *Foxg1*^{Cre}; *Shh*$^{lox/-}$ mutants, our results do not preclude the possibility that the reverse gradient of HC differentiation is indirectly caused by the loss of ganglion functions unrelated to *Shh* or *Ngn1*. Nevertheless, the failure of most of the spiral ganglion to reach the developing cochlear duct observed in *Foxg1*^{Cre}; *Shh*$^{lox/-}$ mutants is not likely related to the replacement of one of the *Foxg1* alleles with cre, because *Foxg1* expression is not affected in the spiral ganglion (Fig. S6).

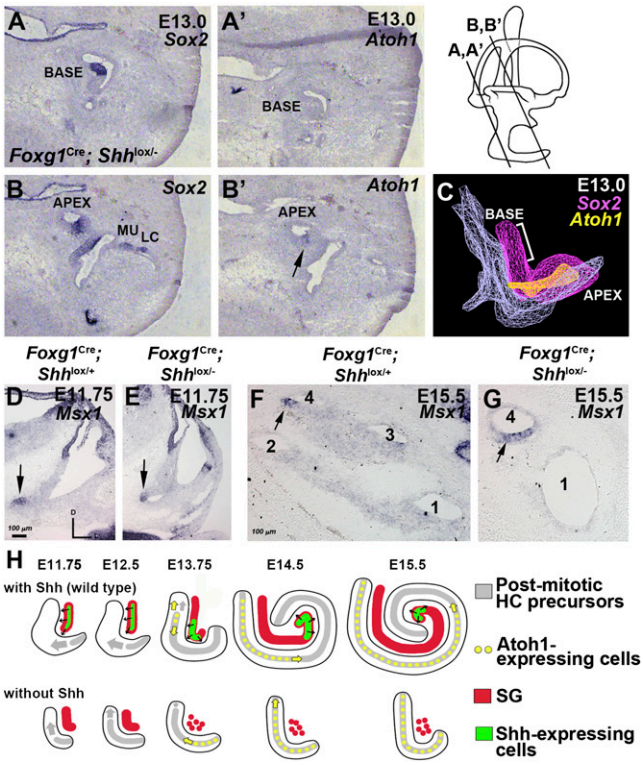

Fig. 5. Expression patterns of *Atoh1* and *Msx1* in *Foxg1*^{Cre}; *Shh*$^{lox/-}$ cochlea. (*A–C*) *Atoh1* expression of *Foxg1*^{Cre}; *Shh*$^{lox/-}$ cochlea at E13. Adjacent sections were probed for *Sox2* (*A* and *B*) and *Atoh1* (*A′* and *B′*) at the base (*A* and *A′*) and apex (*B* and *B′*) of the cochlea. *Atoh1* expression was detected only at the apex within the *Sox2*$^{+}$ prosensory domain (*B′*, arrow). LC, lateral crista; MU, macula utricle. (*C*) A 3D image of *Sox2* (pink) and *Atoh1* (yellow) expression domains in *Foxg1*^{Cre}; *Shh*$^{lox/-}$ cochlea, showing a lack of *Atoh1* expression at the base of the *Sox2*$^{+}$ prosensory domain (bracket). (*D–G*) *Msx1* expression in the ventral tip of the inner ear at E11.75 (*D* and *E*, arrow) and apex of the cochlear duct at E15.5 (*F* and *G*, arrow) of control (*D* and *F*) and *Foxg1*^{Cre}; *Shh*$^{lox/-}$ mutant (*E* and *G*). (*H*) Summary diagram of WT cochlea (*Upper*) showing that Shh, produced in a subpopulation (green) of the spiral ganglion (red), promotes growth of the cochlear duct and inhibition of HC differentiation. As the tip of the cochlear duct extends beyond the reach of Shh, prosensory cells start to exit from cell cycle in that location, after which CCE progresses toward the base. As the cochlear duct continues to grow, *Shh* expression and signaling become restricted toward the apex of the cochlear duct, which allows initiation of HC differentiation at the midbasal region. The lack of Shh causes poor spiral ganglion development and premature CCE, followed promptly by HC differentiation (*Lower*).

Furthermore, the *Foxg1* null cochlea, although shortened as well (23, 24), did not display a similar reverse gradient or up-regulation of *Atoh1* expression (Fig. S7).

What is the relationship among the three roles of spiral ganglion Shh–growth of the cochlear duct, timing of CCE, and timing of HC differentiation? Abnormal organ of Corti development is known to affect cochlear length (25, 26). More importantly, the shortened cochlear duct in *Shh* mutants may simply be the result of precursors prematurely exiting from cell cycle before generating sufficient HCs and even cells outside of the prosensory domain, given that the *Ptc1* expression domain is broader than the prosensory region (Fig. 1 *H–J′*).

The apical-to-basal wave of CCE in $Foxg1^{Cre}$; $Shh^{lox/-}$ mutants suggests that additional factors are involved in establishing this gradient of CCE along the cochlear duct. However, Shh signaling is clearly required for the base-to-apex progression of HC differentiation in the cochlea (Fig. 5*H*). The finding that premature HC differentiation can occur independent of a change in CCE in the $Ngn1^{Cre}$; $Shh^{lox/-}$ mutants suggests that Shh regulates these cellular processes separately.

Atoh1 is the "master" gene identified for specifying HC fate (27). Shh could mediate the timing of HC differentiation by regulating *Atoh1* expression. Shh may promote cell proliferation and inhibit HC differentiation by repressing *Atoh1* expression in the cochlea, in contrast to the positive role of Shh signaling on *Atoh1* in the developing cerebellum (28). Alternatively, Shh may have a dose-dependent effect on *Atoh1* expression in the cochlea, such that *Atoh1* is induced by low doses of Shh at a distance from the ganglion source of *Shh*, but is inhibited close to the source. This scenario is analogous to the situation in the eye disk, in which *atonal* is activated in the morphogenetic furrow, far from the source of hedgehog (where levels are low), but repressed in cells posterior to the furrow close to the source of hedgehog (where levels are high) (29). Whether there is a similar dose-dependent effect of Shh on *Atoh1* expression in the developing cochlea, or whether Shh simply inhibits *Atoh1* in this tissue, requires further study.

In summary, we propose that *Shh* in the spiral ganglion promotes growth of the cochlear duct primarily in the base and midcochlear regions (Fig. 5*H*). As the cochlear duct grows, the apex of the cochlea extends beyond the reach of much of the Shh signaling emanating from the spiral ganglion (reduced *Ptc1* expression in the apex at E13 and E13.5; Fig. 1 *H* and *I*), contributing to the terminal mitosis of apical HC precursors. However, sufficient Shh signaling remains present at the apex to hold off HC differentiation. Although the factors regulating the progression of CCE of HC precursors toward the base are not clear, the premature CCE in both $Foxg1^{Cre}$; $Shh^{lox/-}$ and $Ngn1^{Cre}$; $Shh^{lox/-}$ mutant cochleae suggests that the timing of this progression is under the influence of Shh. In addition, subsequent HC differentiation follows in the wake of restricted *Shh* signaling from the base toward the apex. Thus, the timing of CCE and HC differentiation within the cochlear duct is region-specific, dependent on the proximity of the spiral ganglion source of *Shh*. This continuous feedback integration of Shh signaling from the spiral ganglion and morphogenesis of the cochlear duct may be an evolutionary conserved pathway.

Given the importance of the timing of CCE and differentiation in specifying neuronal subtypes in the central nervous system (7, 8, 30), it is possible that this regulation of CCE and differentiation of cochlear HCs by Shh prefigures the tonotopic organization of this organ.

Materials and Methods

$Ngn1^{457\text{-}Cre}$ mice are designated as $Ngn1^{Cre}$, $Ngn1^{CreERT2}$ are designated as $Ngn1^{CreER}$, and Shh^{tm1Amc} mice (JAX) are designated as $Shh^{+/-}$. Conditional knockouts of *Shh* in the CVG neurons were generated using three different *Cre* strains: $Foxg1^{Cre}$ (from S. McConnell, Stanford University, Stanford, CA), $Ngn1^{CreERT2}$ (from L. Goodrich, Harvard Medical School, Boston), and $Ngn1^{Cre}$ (from J. Johnson, University of Texas Southwestern Medical School, Dallas). Details on paint fills, EdU injection, immunostaining, and cell counts are provided in *SI Materials and Methods*.

ACKNOWLEDGMENTS. We thank Drs. Lisa Goodrich, Jane Johnson, and Susan McConnell for mice and Drs. Lisa Cunningham, Douglas Epstein, Thomas Friedman, Andrew Griffith, James Keller, and Steven Raft for critical reading of the manuscript. This work was supported by the National Research Foundation of Korea (Grants 2011-0028066 and 2012R1A1A2041348, to J.B.) and the National Institute on Deafness and Other Communication Disorders Intramural Program (D.K.W.).

1. Corwin JT, Warchol ME (1991) Auditory hair cells: Structure, function, development, and regeneration. *Annu Rev Neurosci* 14:301–333.
2. Lim DJ (1980) Cochlear anatomy related to cochlear micromechanics: A review. *J Acoust Soc Am* 67(5):1686–1695.
3. Mann ZF, Kelley MW (2011) Development of tonotopy in the auditory periphery. *Hear Res* 276(1-2):2–15.
4. Lee YS, Liu F, Segil N (2006) A morphogenetic wave of p27Kip1 transcription directs cell cycle exit during organ of Corti development. *Development* 133(15):2817–2826.
5. Ruben RJ (1967) Development of the inner ear of the mouse: A radioautographic study of terminal mitoses. *Acta Otolaryngol* 220:220, 1–44.
6. Chen P, Johnson JE, Zoghbi HY, Segil N (2002) The role of Math1 in inner ear development: Uncoupling the establishment of the sensory primordium from hair cell fate determination. *Development* 129(10):2495–2505.
7. Livesey FJ, Cepko CL (2001) Vertebrate neural cell-fate determination: Lessons from the retina. *Nat Rev Neurosci* 2(2):109–118.
8. McConnell SK, Kaznowski CE (1991) Cell cycle dependence of laminar determination in developing neocortex. *Science* 254(5029):282–285.
9. Tabata T, Takei Y (2004) Morphogens, their identification and regulation. *Development* 131(4):703–712.
10. Bok J, Bronner-Fraser M, Wu DK (2005) Role of the hindbrain in dorsoventral but not anteroposterior axial specification of the inner ear. *Development* 132(9):2115–2124.
11. Bok J, et al. (2007) Opposing gradients of Gli repressor and activators mediate Shh signaling along the dorsoventral axis of the inner ear. *Development* 134(9):1713–1722.
12. Riccomagno MM, Martinu L, Mulheisen M, Wu DK, Epstein DJ (2002) Specification of the mammalian cochlea is dependent on Sonic hedgehog. *Genes Dev* 16(18): 2365–2378.
13. Liu Z, Owen T, Zhang L, Zuo J (2010) Dynamic expression pattern of Sonic hedgehog in developing cochlear spiral ganglion neurons. *Dev Dyn* 239(6):1674–1683.
14. Driver EC, et al. (2008) Hedgehog signaling regulates sensory cell formation and auditory function in mice and humans. *J Neurosci* 28(29):7350–7358.
15. Goodrich LV, Johnson RL, Milenkovic L, McMahon JA, Scott MP (1996) Conservation of the hedgehog/patched signaling pathway from flies to mice: Induction of a mouse patched gene by Hedgehog. *Genes Dev* 10(3):301–312.
16. Hébert JM, McConnell SK (2000) Targeting of cre to the Foxg1 (BF-1) locus mediates loxP recombination in the telencephalon and other developing head structures. *Dev Biol* 222(2):296–306.
17. Koundakjian EJ, Appler JL, Goodrich LV (2007) Auditory neurons make stereotyped wiring decisions before maturation of their targets. *J Neurosci* 27(51):14078–14088.
18. Quiñones HI, Savage TK, Battiste J, Johnson JE (2010) Neurogenin 1 (Neurog1) expression in the ventral neural tube is mediated by a distinct enhancer and preferentially marks ventral interneuron lineages. *Dev Biol* 340(2):283–292.
19. Ma Q, Chen Z, del Barco Barrantes I, de la Pompa JL, Anderson DJ (1998) neurogenin1 is essential for the determination of neuronal precursors for proximal cranial sensory ganglia. *Neuron* 20(3):469–482.
20. McKenzie E, Krupin A, Kelley MW (2004) Cellular growth and rearrangement during the development of the mammalian organ of Corti. *Dev Dyn* 229(4):802–812.
21. Tilney LG, Tilney MS, DeRosier DJ (1992) Actin filaments, stereocilia, and hair cells: How cells count and measure. *Annu Rev Cell Biol* 8:257–274.
22. Matei V, et al. (2005) Smaller inner ear sensory epithelia in Neurog 1 null mice are related to earlier hair cell cycle exit. *Dev Dyn* 234(3):633–650.
23. Hwang CH, Simeone A, Lai E, Wu DK (2009) Foxg1 is required for proper separation and formation of sensory cristae during inner ear development. *Dev Dyn* 238(11): 2725–2734.
24. Pauley S, Lai E, Fritzsch B (2006) Foxg1 is required for morphogenesis and histogenesis of the mammalian inner ear. *Dev Dyn* 235(9):2470–2482.
25. Grimsley-Myers CM, Sipe CW, Géléoc GS, Lu X (2009) The small GTPase Rac1 regulates auditory hair cell morphogenesis. *J Neurosci* 29(50):15859–15869.
26. Montcouquiol M, et al. (2003) Identification of Vangl2 and Scrb1 as planar polarity genes in mammals. *Nature* 423(6936):173–177.
27. Zheng JL, Gao WQ (2000) Overexpression of Math1 induces robust production of extra hair cells in postnatal rat inner ears. *Nat Neurosci* 3(6):580–586.
28. Flora A, Klisch TJ, Schuster G, Zoghbi HY (2009) Deletion of Atoh1 disrupts Sonic Hedgehog signaling in the developing cerebellum and prevents medulloblastoma. *Science* 326(5958):1424–1427.
29. Domínguez M (1999) Dual role for Hedgehog in the regulation of the proneural gene atonal during ommatidia development. *Development* 126(11):2345–2353.
30. Desai AR, McConnell SK (2000) Progressive restriction in fate potential by neural progenitors during cerebral cortical development. *Development* 127(13):2863–2872.